Engineering Physics
2022; 6(1): 13-19
http://www.sciencepublishinggroup.com/j/ep
doi: 10.11648/j.ep.20220601.13
ISSN: 2640-1010 (Print); ISSN: 2640-1029 (Online)

Laser Beam Joining of the Material Pairings Aluminum/Polyamide and Aluminum/Polyvinylchloride

Christian Lamberti[1, *], Peter Böhm[2]

[1]Nuform – Venture of Abacus Alpha GmbH, Trierweiler, Germany

[2]Department of Technology, University of Applied Sciences, Trier, Germany

Email address:
christian.lamberti@nuform.eu (C. Lamberti), boehm@fh-tier.de (P. Böhm)

[*]Corresponding author

To cite this article:
Christian Lamberti, Peter Böhm. Laser Beam Joining of the Material Pairings Aluminum/Polyamide and Aluminum/Polyvinylchloride. *Engineering Physics*. Vol. 6, No. 1, 2022, pp. 13-19. doi: 10.11648/j.ep.20220601.13

Received: May 1, 2022; **Accepted**: May 25, 2022; **Published**: June 30, 2022

Abstract: The article presents a process optimization of laser beam joining of the material pairings EN AW-6082 (AlSi1MgMn)/polyamide 6.6 and EN AW-6082/polyvinylchloride hard. The materials selection focuses on their distinct mechanical and electrical properties. Al and PA-6.6 are both widely used but dissimilar light-weighting materials for engineering applications, while Al and PVC represent the combination of a weldable electrical conductor with typical insulation material. The contrariety of these materials potentially acts complementary as highly integrated hybrid structures. However, this dissimilarity also poses distinct challenges to joining polymers with metals. Usually, the material pairing aluminum/plastic has been bonded for industrial applications in the recent past. The investigations provide information on the influence of various parameters on the joint and the individual joining partners themselves and which combination offers the best joining results. In addition, it is shown that specific pre-treatment methods of the test materials, especially for aluminum, can significantly increase the joining quality and offer further optimization potential. Furthermore, the complexity of such an optimization process becomes apparent because it is not only limited to the parameter variation of the laser. The periphery design, such as the sample clamping and the pre-treatment of the joining partners, are similarly essential adjustment parameters. The laser-joined specimens are compared in a tensile test against conventionally bonded specimens for their mechanical-technological properties. It can be shown that the shear strength of joined specimen is significantly higher in comparison to the bonded specimen. Thereby an alternative to conventional bonding processes can be offered. Moreover, the extremely short process time of laser beam joining combined with instant handling is particularly attractive for industrial applications. The laser joining process described in this article aims to contribute to the future development of laser-based multi-material additive manufacturing technologies. In this way, the envisioned direct joining principle could enable the production of highly integrated parts of unseen complexity.

Keywords: Laser Beam Joining, Aluminum/Plastics, Comparison to Conventionally Bonded Samples

1. Introduction

Technological progress is constantly generating new processes and methods in order to be able to implement existing processes better and more efficiently. In this context, resource conservation and energy efficiency are playing an increasingly important role for lightweight solutions pioneering in the future. In order to implement these solutions, it is often necessary to pair different materials, which are then combined in such a way that their properties are optimally exploited in relation to the application. Up to now, the corresponding component parts were often joined by adhesives, even though this can be critical in terms of production and - in the case of later use - aging. Technologies such as laser beam joining are therefore becoming increasingly important. These are successfully used today to produce hybrid components (components made of very different materials) in the automotive, aerospace and aeronautics industries for an increasing number of applications [1].

Furthermore, laser beam joining allows extremely short process times with instant handling and works almost wear-free - both good prerequisites for automation. In addition,

the laser direct joining technology provides a significant leap towards sustainable product creation and a reduction of energy-intensive resources. Plastics can be joined to metals without needing a third medium, such as adhesives, which is an excellent advantage in the subsequent recycling process of hybrid components since fewer materials have to be separated. The wide range of plastics enables a variety of applications to be covered.

Recent advances in additive manufacturing technology have highlighted the benefits of pairing highly dynamic laser sources with the sophisticated raw material handling of the powder bed principle [2]. In conjunction with apparent leaps in developing multi-material recoaters [3], understanding the underlying principles of the laser direct joining polymers [4-8] with metals can potentially exploit endless possibilities, such as complex multi-material components with functional grading and 3-D integrated circuits (3-D IC). Such technology will ultimately reduce waste material and maximize productivity for parts of the highest complexity.

2. Experimental Setup/Experimental Procedure

Figure 1. *Trumpf TruLaser Station 5005.*

The tests were performed on a Trumpf TruLaser Station 5005, Figure 1, with a working plane of 300 mm × 300 mm and a vertical travel distance of 500 mm. The maximum travel speed of the coordinate table is 6 m/min with a positioning accuracy of 0.1 mm. A "TruFiber 500" solid-state laser with an Nd:YAG fiber was used as the beam source. The laser system with a fiber diameter of 22 µm used for the work described here is characterized by very high beam quality and enables highly dynamic welding processes. The focal point diameter is about 21 µm. The installed laser beam optics has programmable focusing optics and is suitable for welding and drilling. The advantage of this system is its generously usable working space with simultaneous dynamic beam guidance. During the tests, the laser beam was spatially modulated. This means that the mirror optics deflects the laser beam onto a circular path with the radius Rx, while at the same time, the coordinate table moves with a linear feed. This has the advantage of creating a wider melt pool while maintaining the energy density of the focused laser beam. In this way, it is possible to break through the oxide layer of the aluminum, as this has a melting point of about 2072°C, and to maintain a stable deep welding process in the metal.

The following parameters were varied during the experiments: Laser beam power P [W], feed rate F [mm/min], modulation radius Rx [mm], modulation speed v [mm/s], focus position offset z [mm]. Figure 2 shows a schematic representation of the movement of the laser beam over the programmable laser optics with a simultaneous forward movement of the coordinate table on which the sample is clamped.

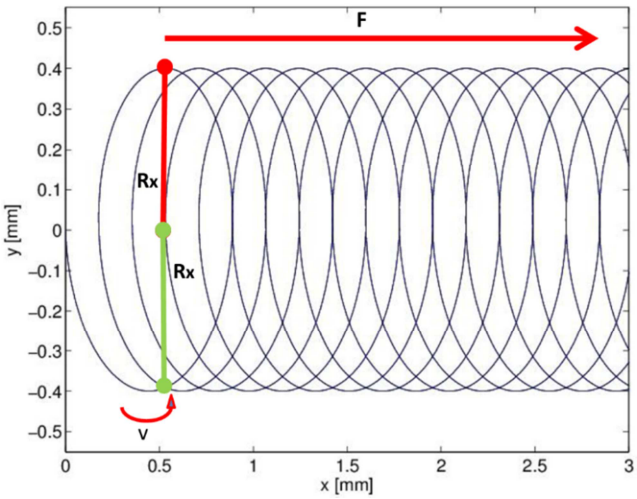

Figure 2. *Schematic drawing of the movement of the laser beam during joining process; movement of the x-y working plate b with velocity F and simultaneous circular motion of the laser beam with radius Rx and velocity v.*

For laser joining of the aluminum with the plastic component, both sheets are overlapped on top of each other, Figure 3. The laser beam (LB) impinges on the aluminum component on the opposite side of the planned joining area and creates a melting area with a key hole (KH) that does not penetrate the aluminum component through its entire thickness and continues along the planned seam path.

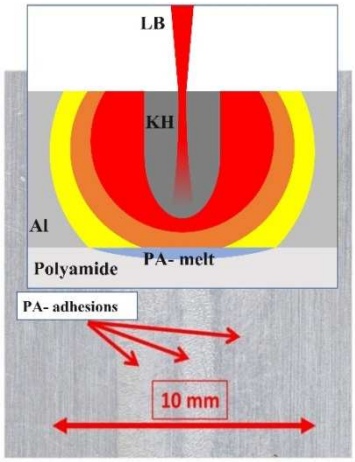

Figure 3. *Schematical drawing of the heat transfer of the molten aluminum with simultaneous view of the detached aluminum specimen with PA adhesions: KH – key hole, LB – laser beam, Al – Aluminum, PA – polyamide.*

Punching through the aluminum component and direct irradiation of the laser beam on the plastic component must be avoided. The heated area of the aluminum component that is in contact with the plastic part also melts the plastic part in the joining zone (PA- melt), causing the aluminum surface to be wetted by the molten plastic. With cooling, an adhesive bond is formed between the two parts. Both parts have a melting area. However, since the melts do not come into contact with each other and do not mix - which would not be possible in terms of the material - this connection is not a welded connection. Due to the joining mechanism of adhesion, such joints are classified as adhesives. Figure 4 shows a scanning electron beam microscope image of a transverse section of a laser-beam joined joint of aluminum with PA 6.6. It can be seen that a gap-free joining surface was achieved. Furthermore, the depth of the melted area in the aluminum sheet is visible and marked with SN. The effects of unintentional melting through the aluminum component resulting in direct contact between the molten aluminum with the plastic will be discussed later. After each laser beam joining of a sample, it was then separated to assess the quality of the bond and the joining areas between the two materials. Based on this information, the previously mentioned parameters were adjusted. For promising parameters, appropriate samples were prepared for tensile testing and metallographic examination. In order to remove coarse surface contaminants on the plastic surface, the PA and PVC specimens were sanded with sandpaper (P1200) and cleaned with isopropanol immediately before the joining process. The tensile specimens were overlapped over a length of 20 mm and joined in the center, Figure 5. The aluminum sheet was cut wider than the polyamide part to achieve pre- or post-heating, which increased the joining area.

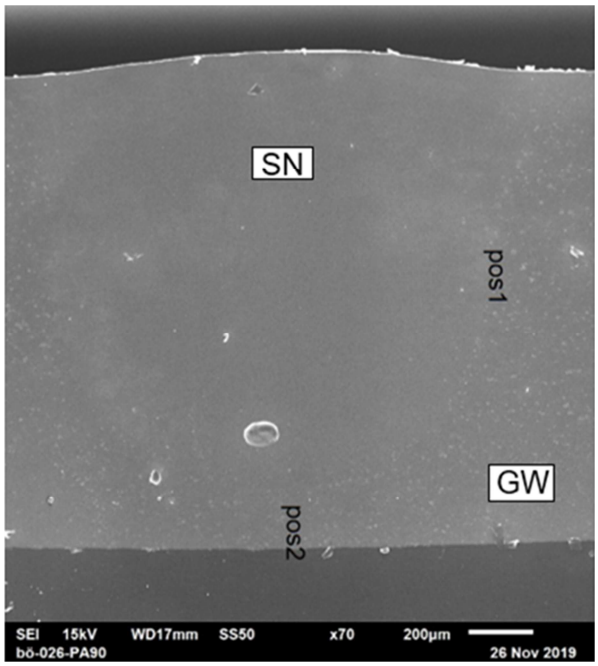

Figure 4. *Recording of a scanning electron microscope showing a laser beam joint of aluminum (light gray) and polyamide 6.6 (dark grey); SN – welded joint, GW-basic material: SN – weld seam, GW – base material.*

Figure 5. *Plan view of the laser beam joint between aluminum and polyamide 6.6.*

3. Results in Lap Joint Aluminum/ Polyamide 6.6

The best results of the aluminum-polyamide compound were obtained with the line energy (E_s) of 8.88 J/mm according to the equation $E_s = P/F$ [J/mm] (P - power, F - feed rate). Furthermore, the selected parameter combination prevented or minimized defects in the melting region of the aluminum, such as cracks and pores. However, the latter cannot always be avoided due to the hydrogen affinity of the aluminum melt and the non-melting through of the aluminum sheet [9]. Adjusting the power to 370 W, in conjunction with an increased modulation speed, resulted in more homogeneous melting across the entire seam width, preventing re-melting. The melt pool was exhibiting a tendency towards inhomogeneity in previous parameter combinations with lower power, lower feed rate and lower modulation speed, which was reflected in an increased number of defects in the aluminum. The degassing possibility of the metallic melt with the optimized parameters is improved by a funnel-shaped formation of the steam capillary. The capillary no longer forms perpendicular to the surface at the increased modulation speed but flattens out slightly. This inclination of the vapor capillary against the feed direction inevitably leads to performance losses. However, the resulting funnel-shaped formation of this channel has a larger cross-section, which makes it easier for the gases to rise up to the melt pool surface. In addition, with a funnel shape, the melt gases are pressed into the melt to a lesser extent by the metal vapors generated in the vapor capillary, which also favors pressure equalization [10]. The described laser beam guidance addressed both significant aspects, the determination of the exact melting depth of the laser beam into the aluminum sample and the avoidance of occurring defects such as hot cracks or pores in the aluminum, Figure 6. A critical factor, which - with both aluminum and polyamide - leads to a poor seam surface, among other things, is melting through the aluminum sheet. In this case, the molten aluminum comes into direct contact with the plastic, which then evaporates abruptly. This phenomenon results in large inhomogeneities in the joint, as parts of the melt are ejected upwards by the resulting gases.

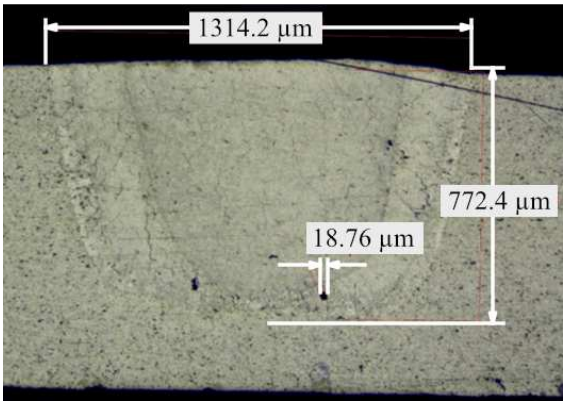

Figure 6. *Cross section of the aluminum specimen presenting the penetration depth in the aluminum sheet and optimized heat transfer as well as a molten area with no defects.*

In some cases, parts of the polyamide melt push through the channels created in this way. To prevent this, either the output must be reduced or the feed rate increased. If the feed rate is increased, however, the speed of the beam oscillation must be increased in equal measure, as described above. Good results can be obtained if the laser beam is adjusted exactly with one revolution of its circular motion with one-tenth of a millimeter feed of the coordinate table. The following formula approximates the link between the ratio of the feed and the welding speed to the oscillating laser beam trajectory.

$$(F - 2\pi - Rx) / (60v) \approx 0.1 \text{ mm} \qquad (1)$$

F - table feed, v - speed of beam oscillation, Rx - modulation radius.

Furthermore, polyamide residues can be detected for the first time on the aluminum surface after the joint has been separated, presumably the primary indication of the improved bonding. The appropriate changes in the parameters also resulted in a detected change in the formation of bubbles in the polyamide melt bath. The bubbles no longer appear as large and scattered but have a smaller and much more finely branched structure, which is also reflected in the polyamide residues on the aluminum surface. The bubble formation is not exclusively restricted to the middle of the plastic melt pool but extends to the melted area's peripheral zones. This widespread suggests a more uniform heat input across the entire width of the melt zone caused by the deeper melting in the aluminum and the shorter process time. The shorter distance from the root bed to the contact surface of the aluminum part with the plastic allows a more concentrated and intensive heat transfer, Figure 7. The better bonding results are also reflected in the joining surfaces. These are more homogeneous over a wider area and do not have any gaps as before. No further bubble formation can be detected in the polyamide melt bath, apart from few exceptions. The improved bond quality could be explained by the short process time of 0.6 s combined with the high power. The low bead formation in the start-up and shut-down zones suggests that the polyamide is only melted in its uppermost layers. Thus, only a minimal amount of polyamide is plasticized, which reduces the formation of potential water vapor during melting [11, 12]. Furthermore, the width of the plastic melt pool is smaller compared to lower feed rates, which is attributed to the resulting shorter time of effective heat input [13].

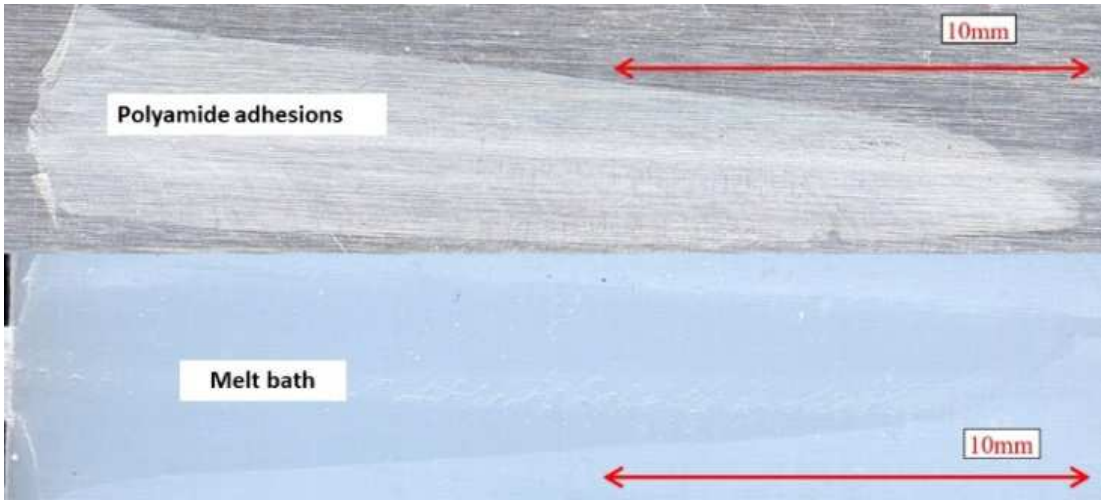

Figure 7. *Upper char - polyamide adhesions on the aluminum surface; lower chart-visible formerly melt bath on the polyamide surface.*

As a result, the contact pressure is distributed over less plasticized polyamide, which presumably promotes the formation of adhesion forces since there is more contact between the joining surfaces. In addition, the formation of bubbles can be minimized in case of high contact pressure since it counteracts the expansion of the gases in the plastic melt [14].

Furthermore, the joining quality could be improved by a special surface pretreatment of the aluminum samples, enhancing the surface wettability. In purely qualitative terms, the wettability is shown in Figure 7. With the aluminum surfaces prepared in this way, it was possible to increase the tensile force of the laser-joined aluminum/PA-6.6 specimens from 1,150 N to 1,800 N, Figure 8, which corresponds to a calculated shear stress of 33.48 N/mm^2, Figure 9.

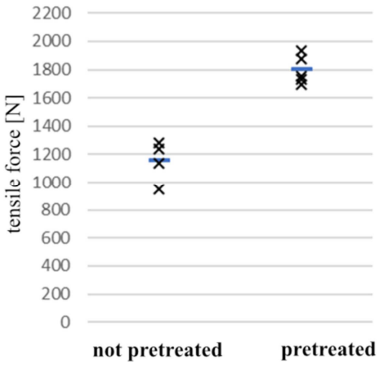

Figure 8. *Increase of the tensile strengths of the laser beam joint by using a special pretreatment of the aluminum surfaces.*

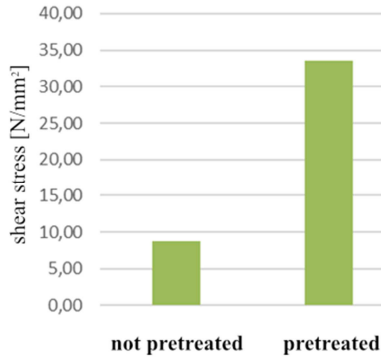

Figure 9. *Increase of the calculated shear stresses of the laser beam joint by using a special pretreatment of the aluminum surfaces.*

4. Results in Lap Joint Aluminum/Polyvinyl Chloride

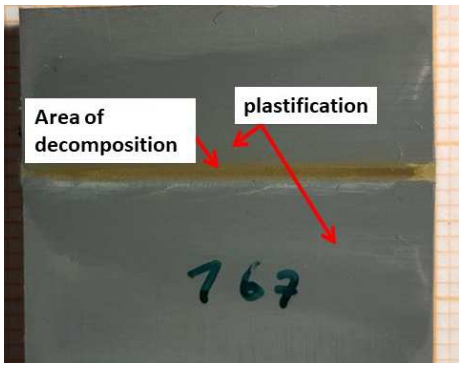

Figure 10. *Polyvinyl chloride residue on the aluminum surface after uncoupling the joint specimen.*

In the case of the Al/PVC material combination, bonding results could only be achieved by thermal decomposition of the polyvinyl chloride. This causes the molten plastic bath to turn yellow, indicating an enrichment with chlorine. Only then are PVC residues also visible on the aluminum after the compound has been separated, Figure 10. Melting the PVC close before its decomposition cannot achieve any bonding. Due to its low melting point of 80°C, plasticization is also visible next to the seam, although the processing time is only 0.6 s. One of the reasons given for the lack of adhesion is that the rapid plasticization of the PVC means that not enough contact pressure can be exerted on the melt for it to adhere to the aluminum. Therefore, adhesion is not achieved with lower feed rates and power combinations.

On the other hand, the decomposition process causes bubbles to form in the middle of the joining zone [15-17]. The resulting increase in the volume of the melt presses it more forcefully against the aluminum surface, enabling better contact to be made. This assumption is also shared by F. Yusof and Y. Miyashita [14, 18]. The bubble formation and decomposition phenomena are exemplified in Figure 11.

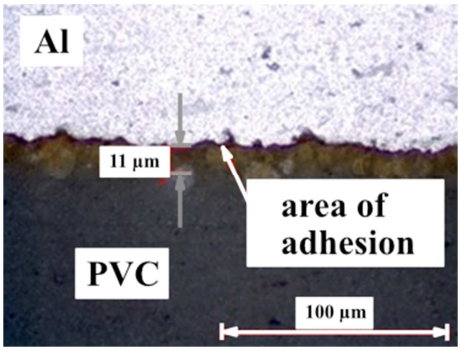

Figure 11. *Cross section of a laser beam joint of aluminum/polyvinyl chloride; the area of degradation is clearly visible at the phase interface as well as the homogenous connection between aluminum/polyvinyl chloride.*

In addition, an EDX analysis shows an enrichment of the chlorine content towards the joining zone, which confirms the assumption of thermal decomposition, Figure 12. The figure presents the scanning direction represented by the green arrow and the element distribution determined simultaneously. The graph shown in red indicates the chlorine content, the green one indicates the aluminum content. In the tensile tests, 530 N for the tensile force and 28.9 N/mm^2 for the shear stress could be achieved. However, when calculating the shear stresses, it must be taken into account that only the de-composed areas of the PVC melt pool have a bonding effect. Thus, the shear stresses were calculated over the bonding area of the PVC residues to the aluminum.

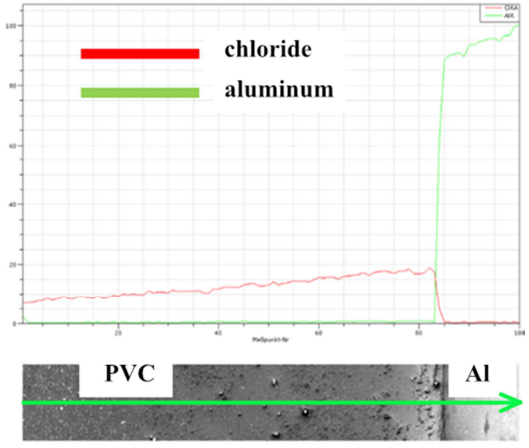

Figure 12. *Distribution of chloride and aluminum within the laser beam joint Al/PVC by means of energy dispersive X-Ray analysis.*

5. Comparison of the Conventionally Bonded and the Laser-Beam Bonded Samples

In order to make a comparison with conventional bonding, both laser-beam bonded and conventionally bonded tensile specimens with the same dimensions were fabricated. The overlap length of the bonded specimens was 20 mm, resulting in a total bond area of 20 mm × 25 mm. The aluminum specimens (raw state) were cleaned with isopropanol, as well as the polyamide and PVC specimens, respectively. The adhesive used was "Loctite 406". The curing time of the adhesive was 48 h at room temperature. Four tensile specimens were prepared for each of the different material pairings. Figure 13 and Figure 14 show the mean values of the results.

Comparing the conventionally bonded specimens with the laser-beam bonded samples, a significant increase in the maximum tensile forces can be observed, especially for the pairing of aluminum and PVC, which is mainly due to the larger joining surface. The lower elongation at break also leads the PVC tensile specimens to perform better than the polyamide tensile specimens, even though both share the same bonded joining area. Overall, the conventionally bonded specimens achieve higher tensile forces. However, the pure tensile forces can only be put into perspective since the bonded area is almost four times as large as the joining area of the laser-beam bonded specimens. The laser-beam joined specimens deliver higher values of shear stress when considering the smaller joining area. The larger, effectively joined area of the conventionally bonded specimens leads to a higher shear stress gradient within the bonded area and thus favors gradual debonding. The laser-beam bonded specimens are also favored in the tensile shear test due to their small effective bond area, which corresponds to the plastic melt pool width. However, this does not affect that high shear stresses can be realized in the smallest space during laser joining by heat conduction.

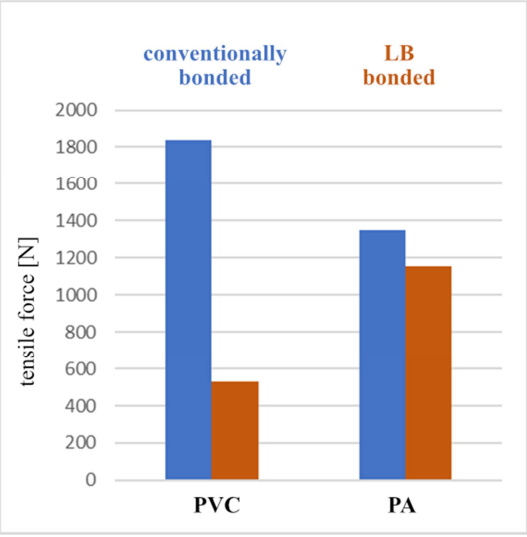

Figure 13. *Comparison of the tensile force of conventionally bonded (blue) and laser beam bonded specimen (brown).*

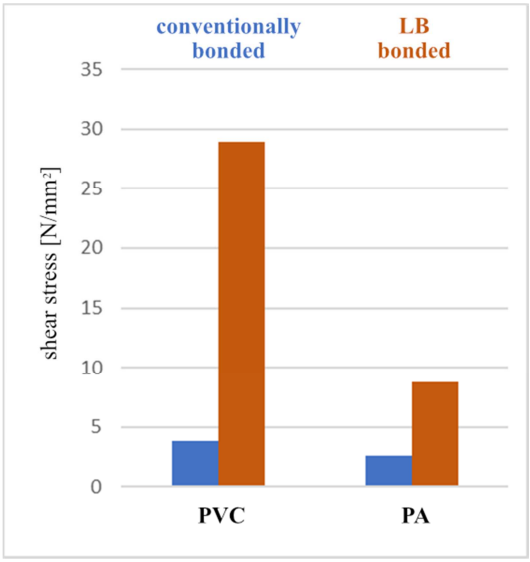

Figure 14. *Comparison of the shear stress of conventionally bonded (blue) and laser beam bonded specimen (brown).*

6. Conclusion

The experiments prove that the production of laser-beam joints of "EN AW-6082/Polyamide 6.6" or "EN AW-6082/PVC-hard" is possible and represents an alternative to conventional bonding. The extremely short process time of laser beam joining combined with instant handling is particularly attractive for industrial applications. The selected parameter combination could almost eliminate the formation of bubbles in the polyamide 6.6 melt bath. Only the surface of the polyamide was melted due to the short process time of 0.6 s. Further enhancements to the joint quality are expected under moisture-controlled conditions by pre-drying the hydrophilic polymer polyamide before the thermal joining procedure [19]. In conjunction with the increased surface energy of the treated aluminum samples, tensile forces of over 1800 N or shear stress of more than 33 N/mm^2 could be achieved. The laser-joined Al/PA specimens thus exhibit much higher values than the conventionally bonded specimens with values averaging 3.5 N/mm^2. As a result of the optimized surface treatment, the plastic melt can better wet the treated aluminum samples due to increased surface energy. Additionally, previous investigations showed that the pre-treatment of the aluminum samples before the laser joining operation affected the formation of chemical modifications such as Al_2O_3, AlO-OH and $(AlOH)_3$ at the aluminum surface [6]. These observations indicate that the increase in surface energy and the presence of reactive groups in the interface promote stronger adhesion.

Shear stresses of up to 28 N/mm^2 could be achieved with the Al/PVC material pairing, which is several times higher than conventionally bonded specimens. However, the bond formation can be traced back to the thermal decomposition process of the PVC. The exact circumstances leading to the measurable increase in the bond strength between the dissimilar materials cannot yet be determined with certainty [20]. It can be speculated that the expanding gases formed in

the decomposition area press the melt more strongly against the aluminum surface, thereby causing more intensive contact between the joining surfaces with an increased adhesive force [17]. On the other hand, the enrichment of the chlorine content within the plastic - towards the joining zone and especially immediately below the aluminum melt zone - correlates with the increase in the breaking force. The extent to which increased formation of adhesive forces is made possible by the mechanisms of functional groups requires further investigation [6].

Concerning developments in additive manufacturing, additional experiments need to elaborate on how the treatment of the metallic partner will reduce the quality of the bulk metallic structure. Surface oxides and compounds such as AlO-OH and $Al(OH)_3$ are expected to compromise the fusion of metallic particles in favor of stronger bonds to the polymer molecule's reactive groups.

References

[1] Temesi, T., Czigány, T. (2020). Integrated Structures from Dissimilar Materials: The Future Belongs to Aluminum-Polymer Joints. Advanced Engineering Materials, 22.

[2] Mehrpouya, M., et al (2022) Rapid Prototyping Journal, Multimaterial powder bed fusion techniques, 28 (11), 1–19.

[3] Amor-Dei-Jabo-Cyusa, J., (2022). Master Thesis, Université de Liège, Optimization and Characterization of Metallic Multi-Materials by Laser Powder Bed Fusion.

[4] Cavezza, F., et al (2019), J. Phys. Chem. C, Probing the Metal Oxide/Polymer Molecular Hybrid Interfaces with Nanoscale Resolution Using AFM-IR, 123, 43, 26178–26184.

[5] Chueh, Y-H., et al (2020). Additive Manufacturing, Additive manufacturing of hybrid metal/polymer objects via multiple-material laser powder bed fusion, 36 (1); 101465.

[6] Lamberti, C., (2018). PhD thesis, University of Luxembourg, Optimierung und Charakterisierung einer mittels Laserstrahl gefügten Verbindung zwischen Aluminium und Polyamid 6.6, 128-129.

[7] Jain, J. K. and Sonia, P. (2022). Recent Trends in Welding Polymers and Polymer–Metal Hybrid Structures. In Light Weight Materials (eds K. Kumar, B. S. Babu and J. P. Davim).

[8] R. Falck, S. M. Goushegir, J. F. dos Santos, S. T. Amancio-Filho, (2018). Materials Letters, AddJoining: A novel additive manufacturing approach for layered metal-polymer hybrid structures, 211-214, 217.

[9] Enz, J., (2012). HZG REPORT 2012-2, Laserstrahlschweißen von hochfesten Aluminium-Lithium Legierungen, 11-13; 68.

[10] Tang, Zuhao, (2014). Strahltechnik, Heißrissvermeidung beim Schweißen von Aluminiumlegierungen mit einem Scheibenlaser, Bd. 53, 3-8, BIAS Verlag.

[11] Amanat, N., Chaminade, C., Grace, J., McKenzie, D. R, James, N. L., (2010). Materials and Design, 31 (10), Transmission laser welding of amorphous and semi-crystalline poly-ether-ketone for applications in the medical device industry, 4823-4830.

[12] Kagan, V. A., Kocheny, S. A., Macur, J. E., (2005). Journal of reinforced plastics and composites, Moisture effects on mechanical performance of laser-welded polyamide.

[13] Schricker, K., et al (2015). Wdg. in the World 59, Experimental investigation and modeling of the melting layer in polymer-metal hybrid structures, 407-412.

[14] Miyashita, Y, (2015). Mechanical Engineering J. 2, Formation behavior of bubbles and its effect on joining strength in dissimilar materials laser spot joining between PET and SUS304, 6.

[15] Jung, K., Kawahito, Y., Takahashi, M., Katayama, S. (2013). Materials and Design, 47, Laser direct joining of carbon fiber reinforced plastic to zinc-coated steel, 179-188.

[16] Jung, K., Kawahito, Y., Katayama, S., (2014). International Journal of Precision Engineering and Manufacturing-Green Technology, Mechanical property and joining characteristics of laser direct joining of CFRP to polyethylene terephthalate, 43-48.

[17] Katayama, S., Kawahito, Y., (2008). Scripa Materialia, 59, Laser direct joining of metal and plastic, 1247-1250.

[18] Yusof, F., Miyashita, X., Seo, N., Mutoh, Y., Moshwan, R. (2012). Science and Technology of Welding and Joining 17, Utilising friction spot joining for dissimilar joint between aluminum alloy (A5052) and polyethylene terephthalate, 544-549.

[19] Lamberti, C, Peral Alonso, I., (2017). Atiner Conference Paper Series No. IND2017-2270, Athens, Influence of Material Moisture during Laser Joining of Polyamide 6.6 to Aluminum.

[20] Farazila, Y., Miyashito, Y., Hua, W., Mutoh, Y., Otsuka, Y., (2011). JLMN-Journal of Laser Micro/Nanoengineering 6 (1), YAG laser spot welding of PET and metallic materials, 69-74.